Appendix to "Parametric study of noise from dual-stream nozzles"

By K. Viswanathan

Journal of Fluid Mechanics, vol. 521 (2004), pp. 35-68

1. Characteristics of turbulent mixing noise

Spectral information over a wide range of angles is presented to illustrate the effects of the parametric variation. When the two streams are operated at sub-critical pressure ratios, one-third octave spectra are presented. The frequencies are represented in terms of band number and in Hertz. The band number is defined as [10*Log_{10} (*f*)], with the center frequency of the 1/3-octave band *f* in Hertz. A non-dimensional frequency in terms of a Strouhal number is not used because of the different velocities (Vp, Vs, or Vmix) and diameters (Dp, Ds, or Dequivalent) that characterize the flow and geometry. When shocks are present in either stream, or when finer details are of interest, narrowband power spectra are shown. Even though the emphasis is on mixing noise in this section, a low supercritical value for the NPR of 2.1 (M=1.09) is also included. As will be seen, a strict distinction between weak and strong shocks in one of the streams is not possible because of the complex mechanism for noise generation. However, the influence of shock-associated noise may be discerned more easily when compared against mixing noise.

First we examine the effect of varying the primary jet conditions, while maintaining the secondary stream at fixed NPR (velocity). In Figures A1 to A3, the secondary nozzle pressure ratios are 1.4, 1.8 and 2.1, respectively. Three conditions for the primary stream are shown at each secondary NPR as follows: NPRp=1.4 and Tp/Ta=2.14, NPRp=1.6 and Tp/Ta=2.26, and NPRp=1.8 and Tp/Ta=2.37. In Figure A1, the velocity ratios (*Vs/Vp*)

are 0.68, 0.57 and 0.5, respectively. At these relatively low velocity ratios, there is a nearly uniform increase in spectral level at the lower angles when the velocity of the primary stream is increased. As we move aft, there is a substantial increase in level near the peak frequency, while the increase at the higher frequencies is comparable to that seen at lower angles. It should be noted that the spectral levels at the last 2 or 3 bands at the aft angles were deemed inaccurate and set to zero. This abrupt drop, seen occasionally, should therefore be disregarded. In Figure A2, the velocity ratios are 0.88, 0.74 and 0.65, respectively. For this set of data, the increase in noise at the higher frequencies is small, ~1 dB at all the angles. Near the peak frequency, there is only a small increase at lower angles while it is more pronounced at aft angles. In the set of data shown in Figure A3, where there is a weak shock in the secondary stream (Ms=1.09), the velocity ratios are much higher: 0.98, 0.82 and 0.72, respectively. The strength of the secondary shear layer (secondary – ambient) is much stronger than that of the inner shear layer (primary – secondary), and it is observed that there is no change in the high-frequency noise when the inner stream is changed. For the sake of completeness, a sample case is shown where the inner shear layer has been removed by operating both the streams pressure balanced and at ambient temperature. Figure A4 shows spectral comparisons with (NPRp=NPRs=1.8, Tp/Ta=2.37) and without (NPRp=NPRs=1.8, Tp/Ta=Ts/Ta=1.0) the inner shear layer. While there are only minor changes in the spectra at low angles, there is a significant increase in levels at the peak frequencies as we move aft. However, the change in spectral levels with increasing velocity in the primary stream and for a fixed secondary velocity is modest at the higher frequencies at all angles. The above three figures confirm that at higher velocity ratios, the secondary shear layer is responsible for the generation of high-frequency noise radiated to all angles. This trend has been noted in past studies, especially by Lu (1983), who investigated the source characteristics and the far-field spectra through the use of an elliptic acoustic mirror, multiple sideline microphone arrays, and two near field microphones for cross-correlation measurements.

The above cases, with either both streams subsonic or with the secondary stream slightly supersonic, establish the importance of the velocity ratio on radiated noise. At low velocity ratios, there is an increase in level across the entire spectrum in the forward quadrant and near-normal angles when the velocity of the primary stream is increased. The magnitude of the increase at the lower angles is also nearly uniform across the spectra, similar to the effect noted in Viswanathan (2002b) where a nearly monotonic increase in level was observed when the velocity of the primary or the secondary stream was increased. At the higher velocity ratios, when the strength of the outer shear layer is much stronger, there is no change in spectral level at the higher frequencies at all angles. However, in the aft directions, there is a substantial increase in noise at the low and mid-frequencies, with the increase more pronounced at lower velocity ratios. It is generally believed that the fully merged jet is responsible for the generation of the low and mid-frequency noise. When the velocity of the primary stream is increased, the velocity of the mixed jet increases, directly leading to an increase in the low frequency noise. This effect can be noted especially in Figure A4.

The effect of varying the secondary jet, while maintaining the primary stream at fixed NPR and temperature (velocity) is examined now. In Figures A5 to A7, the conditions for the primary stream are as follows: NPRp=1.4 and Tp/Ta=2.14, NPRp=1.8 and Tp/Ta=2.37, and NPRp=2.1 and Tp/Ta=2.54, respectively. The pressure ratios in the secondary stream are 1.4, 1.6, 1.8 and 2.1. When the primary stream is subsonic, Figures A5 and A6, the contribution of the shock noise, when the secondary NPR is 2.1, is evident at the lower angles. There is also a nearly uniform increase in level at the lower angles with increasing sub-critical pressure ratio in the secondary stream. There are some interesting trends at the aft angles. In Figure A6, there is no change in the levels at the mid-frequencies, while there is an increase at the low and high frequency regimes. In Figure A7, these trends are more pronounced with an actual reduction in noise in the mid-frequencies, when the secondary pressure ratio is increased. Furthermore, the angular sector where this reduction occurs extends to lower angles, with no change in level at an

angle of 130°. When the NPR in the secondary stream is increased from 1.4 to 2.1 in Figure A7, the mixed velocity increases by ~18% and the thrust increases by ~77%. It is remarkable that there is an actual reduction in noise at the mid-frequencies in the peak radiation direction associated with this change. It should be noted that the bypass ratio increased from 2.67 to 4.65. This trend attests to the complex interplay between source alteration and propagation (flow/acoustic interaction) effects. At the subsonic conditions, at all angles, there is a gradual increase in level at the higher frequencies with increasing secondary velocity, again indicating that the secondary shear layer is responsible for this portion of the generated noise.

The main observations on mixing noise are summarized. The present results confirm the influence of the velocity ratio on mixing noise. At low velocity ratios, there is an increase in level across the entire spectra in the forward quadrant and near-normal angles when either the primary or secondary velocity is increased. At higher velocity ratios, when the strength of the outer shear layer is much stronger, there is no change in spectral level at the higher frequencies at all angles. However, in the aft directions, there is a substantial increase in noise at the low and mid-frequencies, with the increase more pronounced at lower velocity ratios. When the velocity of the primary stream is increased, the velocity of the mixed jet increases, directly leading to an increase in the low frequency noise. At low velocity ratios, when the velocity in the secondary stream is increased with a fixed velocity in the primary stream, there is a reduction in the mid-frequency levels at the aft angles.

These trends are interpreted as follows: (a) the secondary shear layer is responsible for the generation of the high-frequency noise radiated to all angles; (b) the fully merged jet is likely responsible for the generation of the low and mid-frequency noise; (c) an increase in the mixed velocity in itself does not lead to increased noise levels at all angles and complex effects due to flow/acoustic interaction, refraction, shielding, and modifications to source strength govern the noise radiation process.

2. Effect of forward flight on mixing noise

The effect of a tunnel Mach number M_t of 0.2 is shown in Figures A8 and A9. The jet operating conditions are the same as shown in Figures A1 and A3. In Figure A8, the effect of increasing the velocity of the primary stream produces trends very similar to the ones seen for the static case in Figure A1. Again, in Figure A9, identical results are obtained as for the static case shown in Figure A3. Though the overall levels are lower because of the presence of the flight stream, the trends are identical to those of the static cases. The flight effects are shown in Figures A10 and A11 for three free-stream Mach numbers of 0.0, 0.2 and 0.32. The jet conditions for Figure A10 are NPRp=1.6, Tp/Ta=2.26 and NPRs=1.8, while those for Figure A11 are NPRp=1.8, Tp/Ta=2.37 and NPRs=2.1. In Figure A10, there is a decrease of ~5 dB across the spectrum at the lower angle for a tunnel Mach number of 0.2. The spectral levels at the lower angles are very close to that of the noise floor for a tunnel Mach number of 0.32 and hence not shown. As seen in the aft angles, there is a further reduction in noise with an increase in tunnel Mach number. In the principal radiation directions, there is a substantial reduction at the lower frequencies, ~9 to ~13 dB for the two free-stream Mach numbers, while there is only a modest reduction at the higher frequencies. The spectra for the noise floor are also included, which account for the up-turns in the spectra at very low frequencies.

In summary, though the strengths of the different noise sources are reduced in the presence of an external stream, spectral variations due to changes in jet cycle conditions are similar to those observed with no external flow. Secondly, the flight stream causes a substantial reduction in peak noise levels (at lower frequencies) in the aft directions, with a modest reduction at the higher frequencies.

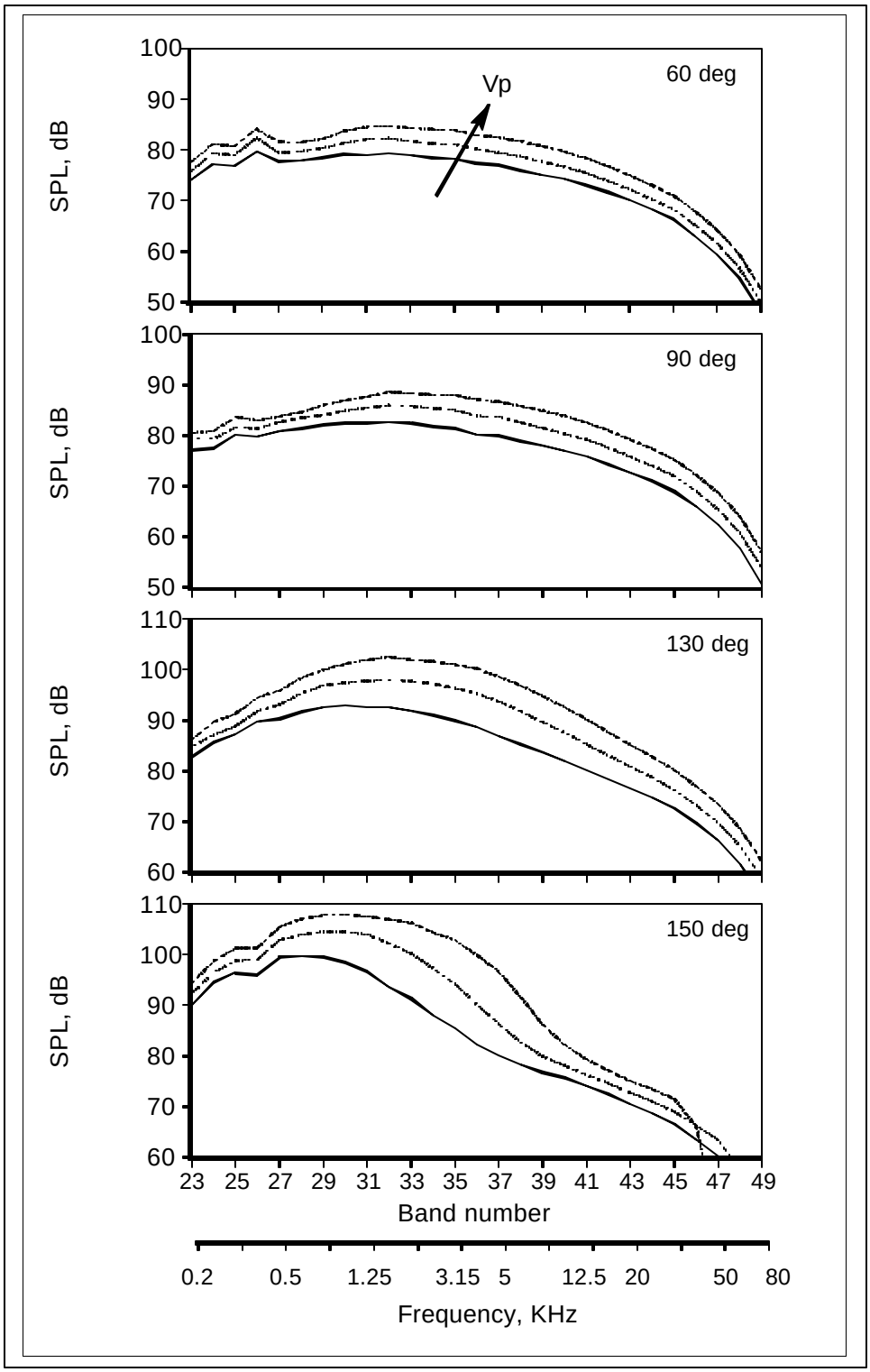

Figure A1. Spectral variation due to change in primary stream with fixed secondary jet conditions. NPRs=1.4, Ts/Ta=1.0. Solid: NPRp=1.4, Tp/Ta=2.14 (Vs/Vp=0.68); dashed: NPRp=1.6, Tp/Ta=2.26 (Vs/Vp=0.57); dot-dashed: NPRp=1.8, Tp/Ta=2.37 (Vs/Vp=0.50).

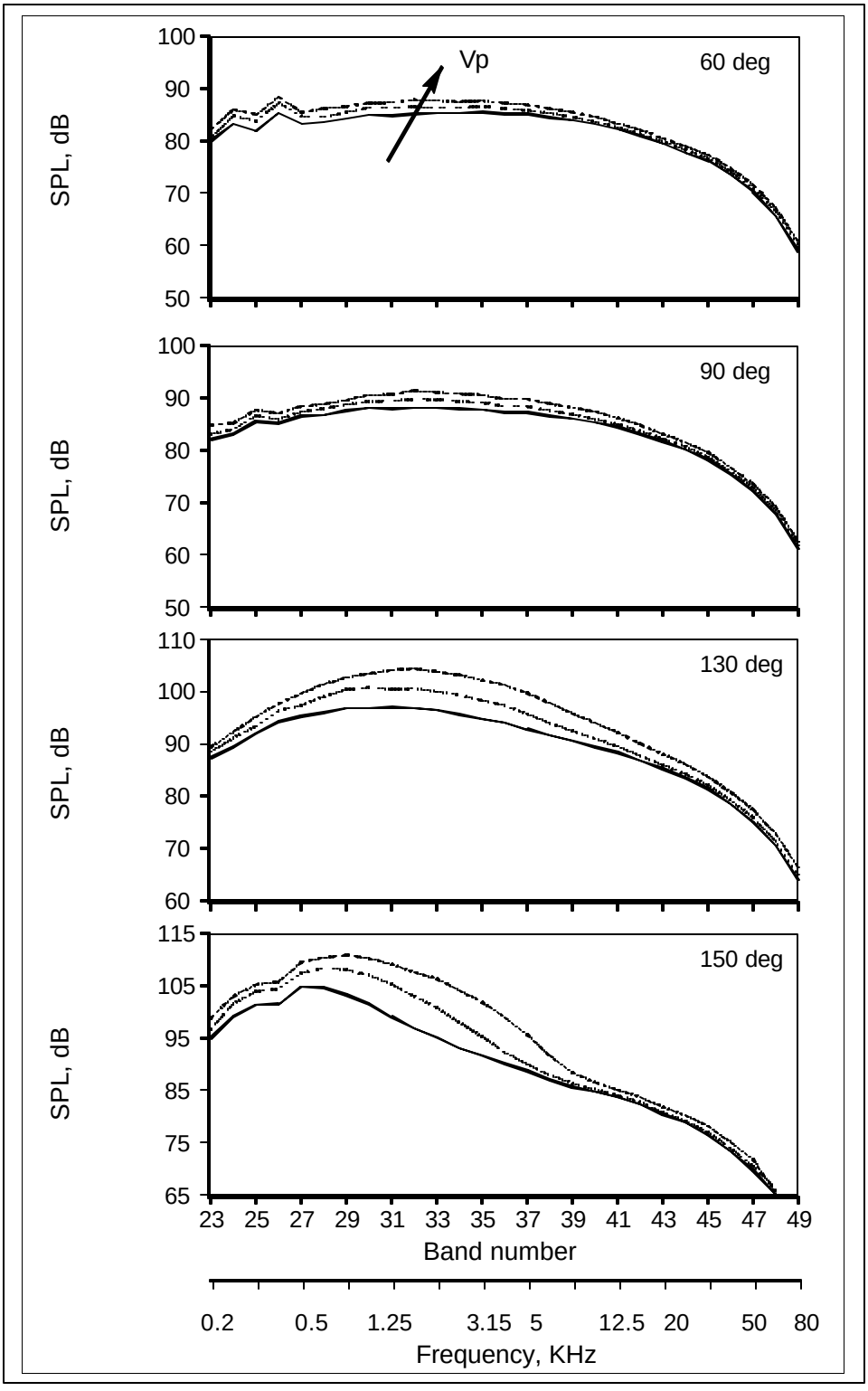

Figure A2. Spectral variation due to change in primary stream with fixed secondary jet conditions. NPRs=1.8, Ts/Ta=1.0. Solid: NPRp=1.4, Tp/Ta=2.14 (Vs/Vp=0.88); dashed: NPRp=1.6, Tp/Ta=2.26 (Vs/Vp=0.74); dot-dashed: NPRp=1.8, Tp/Ta=2.37 (Vs/Vp=0.65).

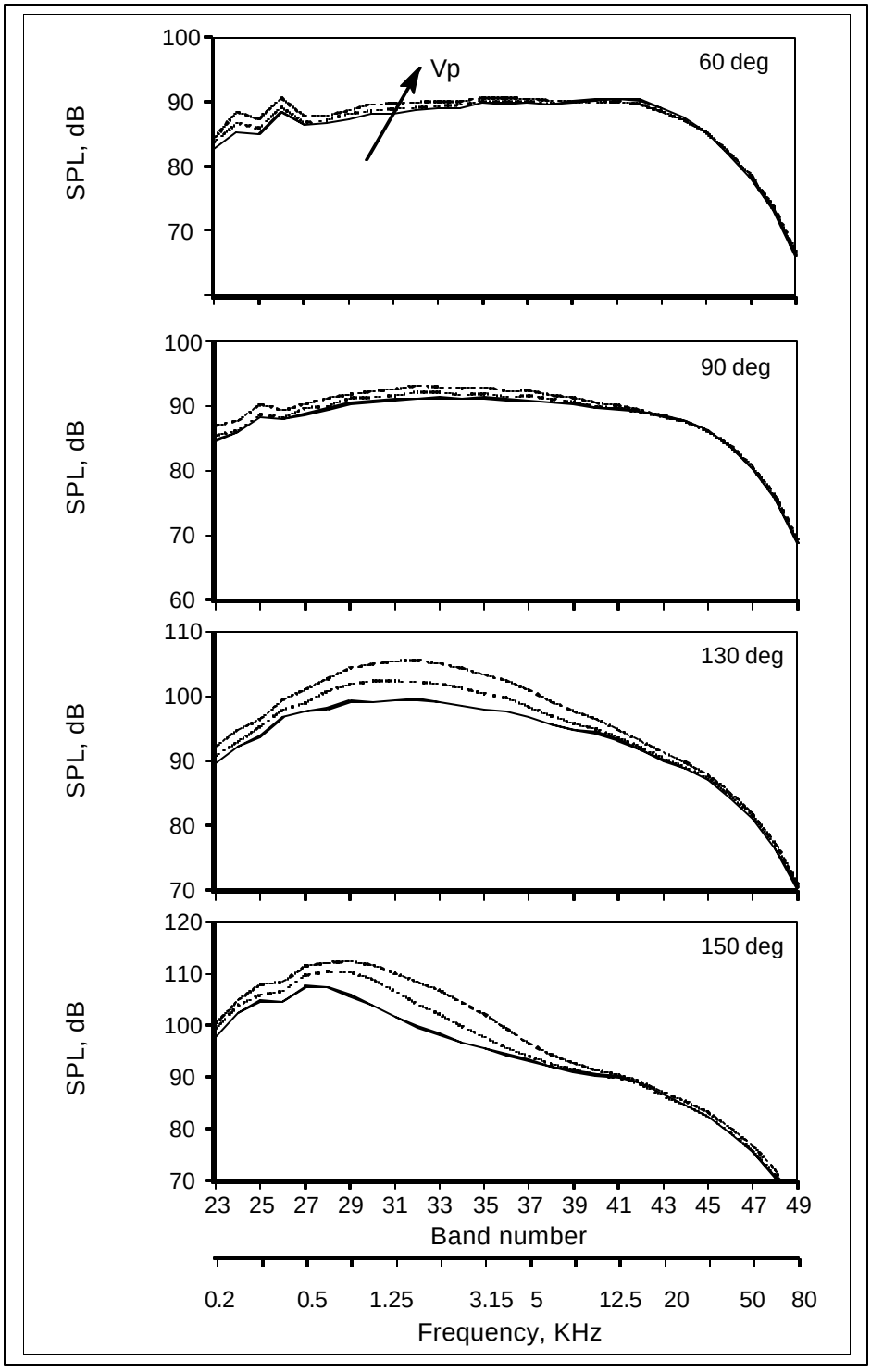

Figure A3. Spectral variation due to change in primary stream with fixed secondary jet conditions. NPRs=2.1, Ts/Ta=1.0. Solid: NPRp=1.4, Tp/Ta=2.14 (Vs/Vp=0.98); dashed: NPRp=1.6, Tp/Ta=2.26 (Vs/Vp=0.82); dot-dashed: NPRp=1.8, Tp/Ta=2.37 (Vs/Vp=0.72).

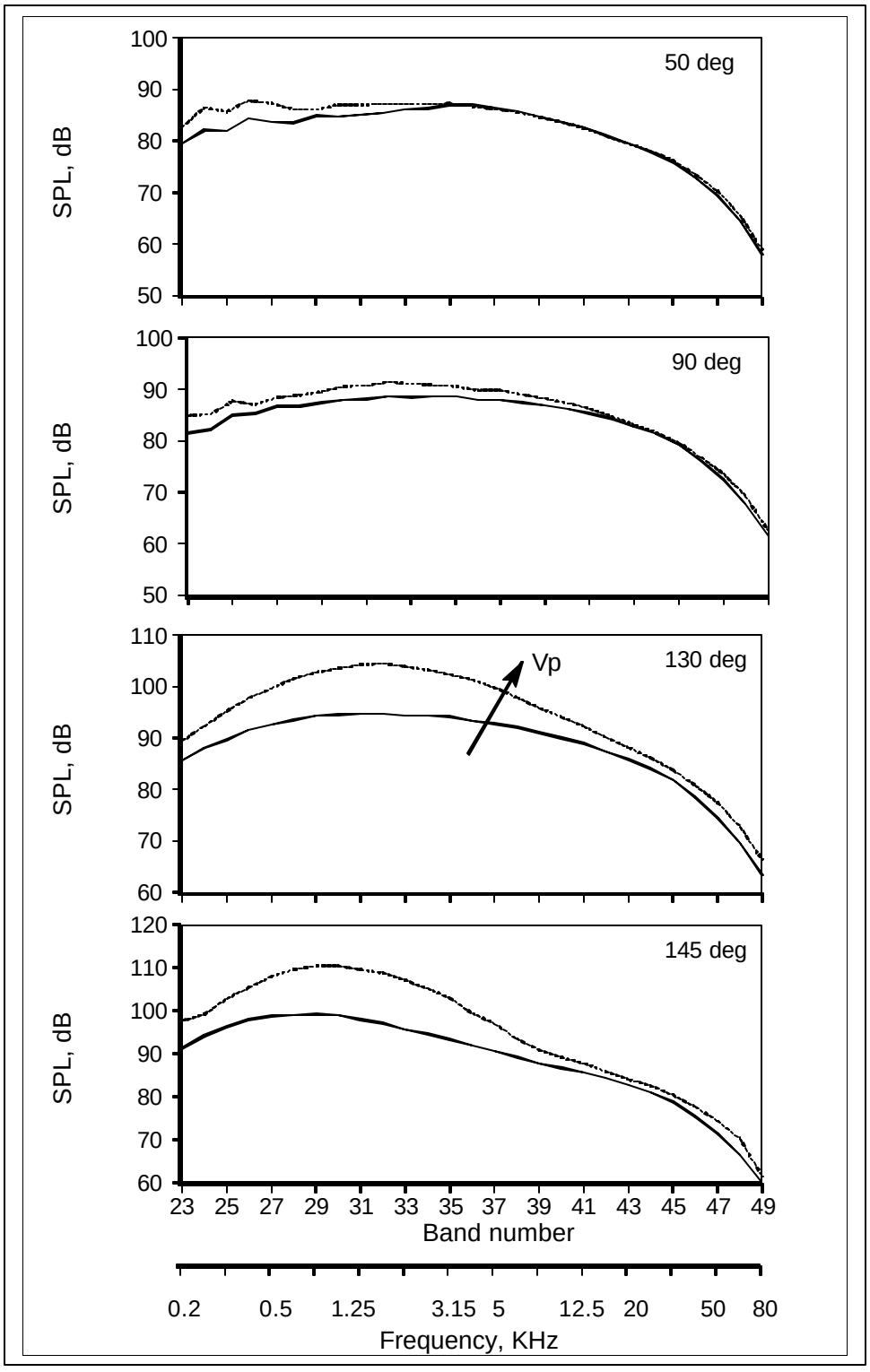

Figure A4. Spectral variation due to change in primary stream with fixed secondary jet conditions. NPRs=1.8, Ts/Ta=1.0. Solid: NPRp=1.8, Tp/Ta=1.0; dashed: NPRp=1.8, Tp/Ta=2.37.

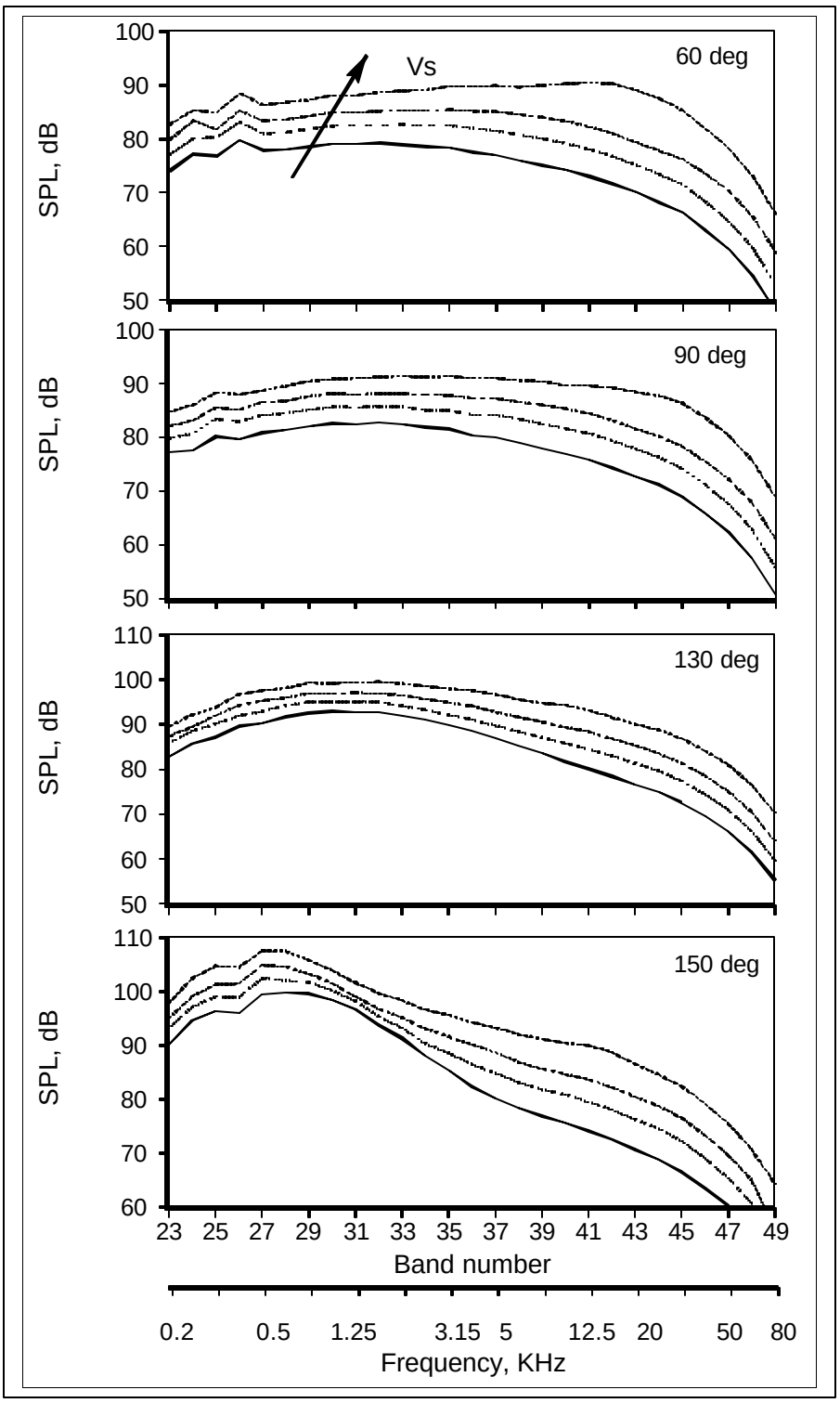

Figure A5. Spectral variation due to change in secondary stream with fixed primary jet conditions. NPRp=1.4, Tp/Ta=2.14, Ts/Ta=1.0. Solid: NPRs=1.4; dotted: NPRs=1.6; dot-dashed: NPRs=1.8; dashed: NPRs=2.1.

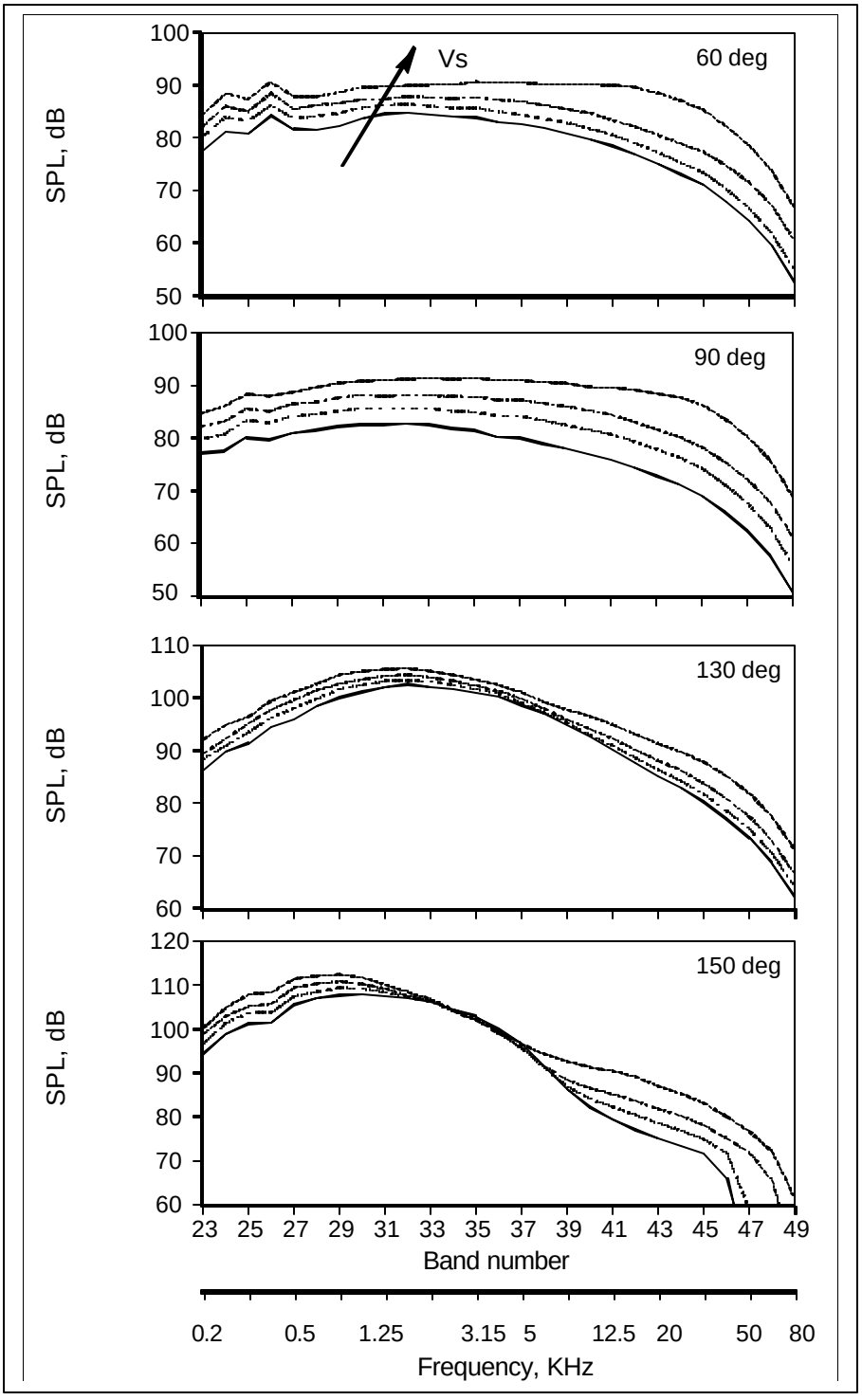

Figure A6. Spectral variation due to change in secondary stream with fixed primary jet conditions. NPRp=1.8, Tp/Ta=2.37, Ts/Ta=1.0. Solid: NPRs=1.4; dotted: NPRs=1.6; dot-dashed: NPRs=1.8; dashed: NPRs=2.1.

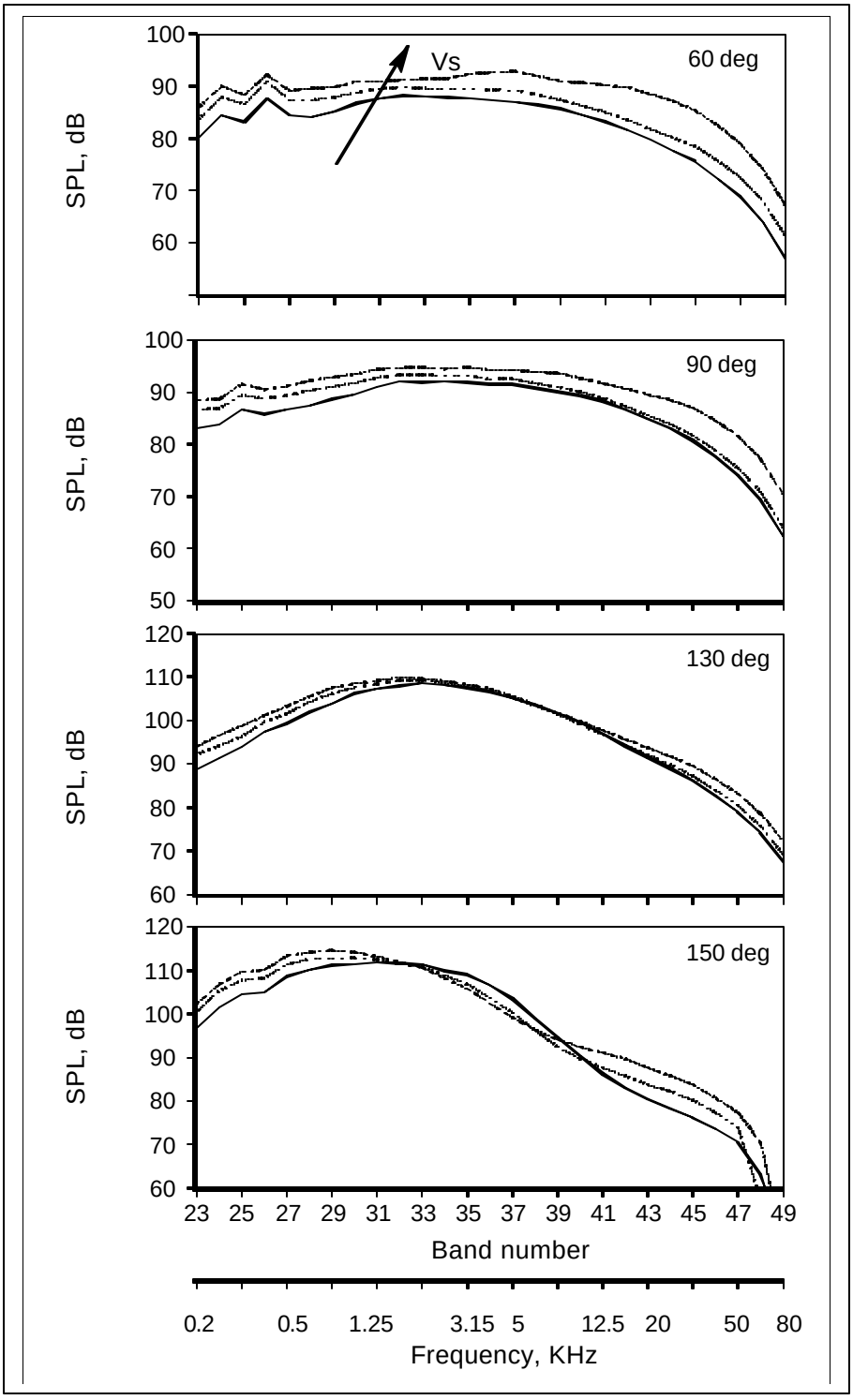

Figure A7. Spectral variation due to change in secondary stream with fixed primary jet conditions. NPRp=2.1, Tp/Ta=2.54, Ts/Ta=1.0. Solid: NPRs=1.4; dotted: NPRs=1.8; dot-dashed: NPRs=2.1.

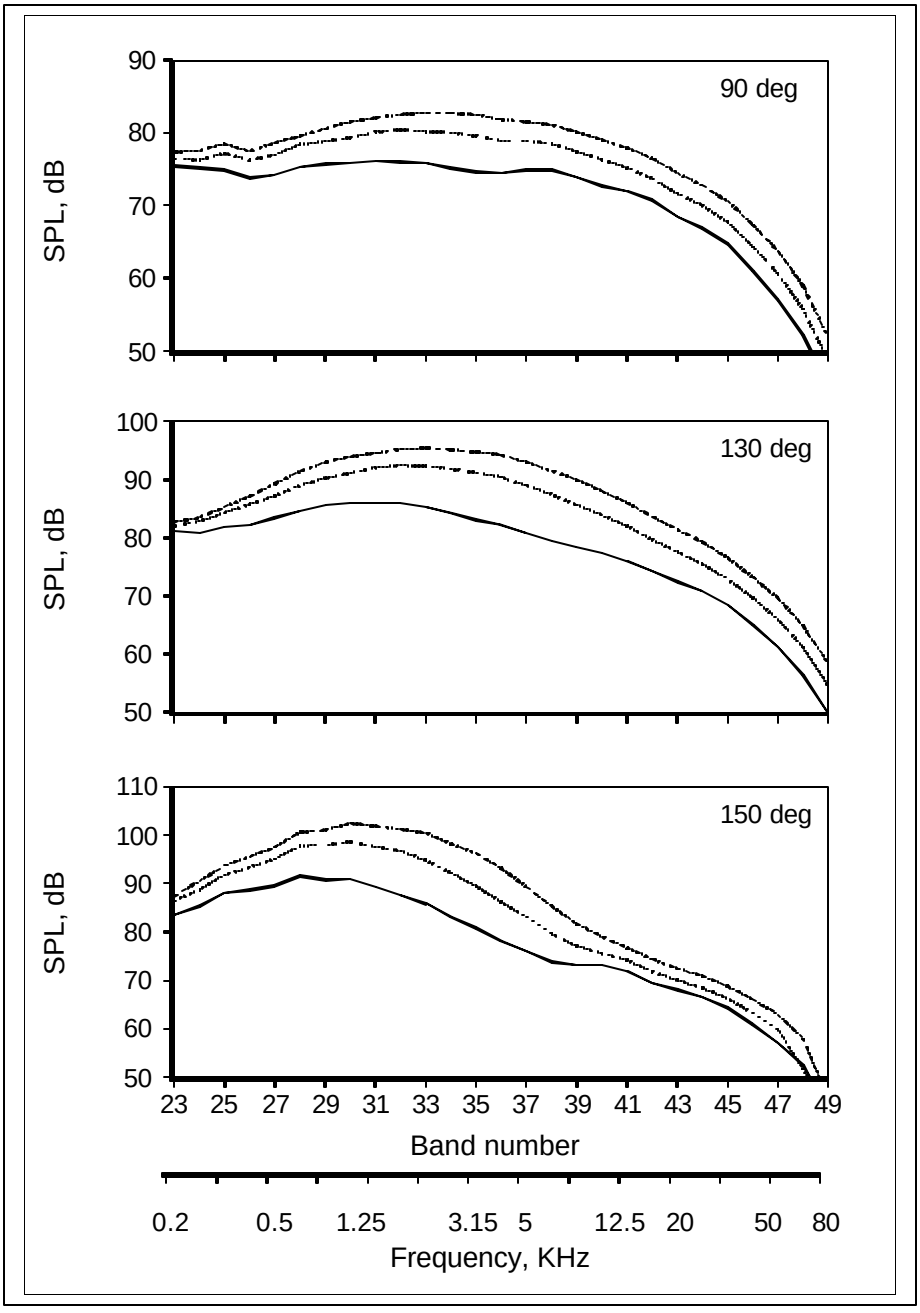

Figure A8. Spectral variation due to change in primary stream with fixed secondary conditions. Mt=0.2. NPRs=1.4, Ts/Ta=1.0. Solid: NPRp=1.4, Tp/Ta=2.14 (Vs/Vp=0.68); dashed: NPRp=1.6, Tp/Ta=2.26 (Vs/Vp=0.57); dot-dashed: NPRp=1.8, Tp/Ta=2.37 (Vs/Vp=0.50).

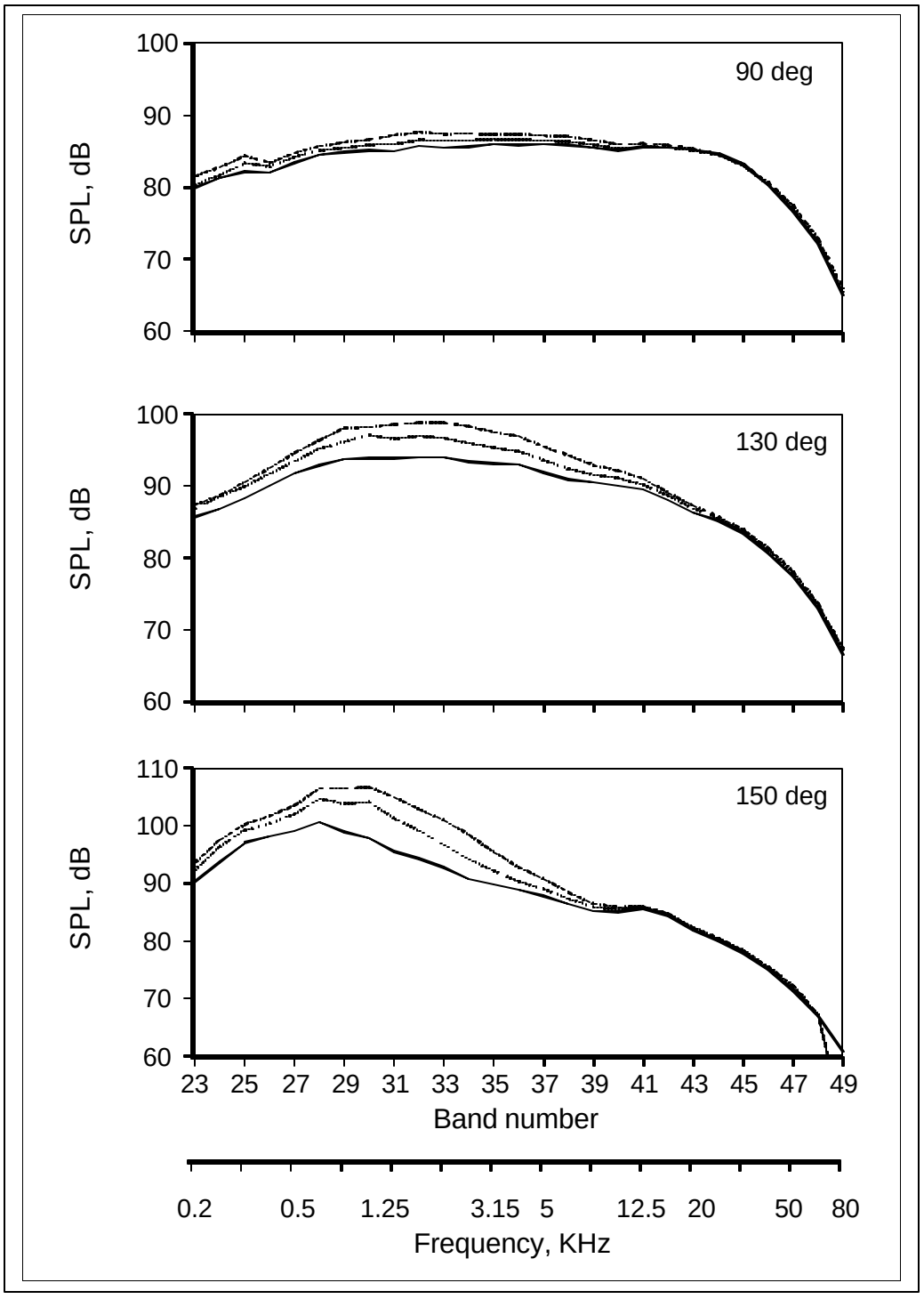

Figure A9. Spectral variation due to change in primary stream with fixed secondary conditions. Mt=0.2. NPRs=2.1, Ts/Ta=1.0. Solid: NPRp=1.4, Tp/Ta=2.14 (Vs/Vp=0.98); dashed: NPRp=1.6, Tp/Ta=2.26 (Vs/Vp=0.82); dot-dashed: NPRp=1.8, Tp/Ta=2.37 (Vs/Vp=0.72).

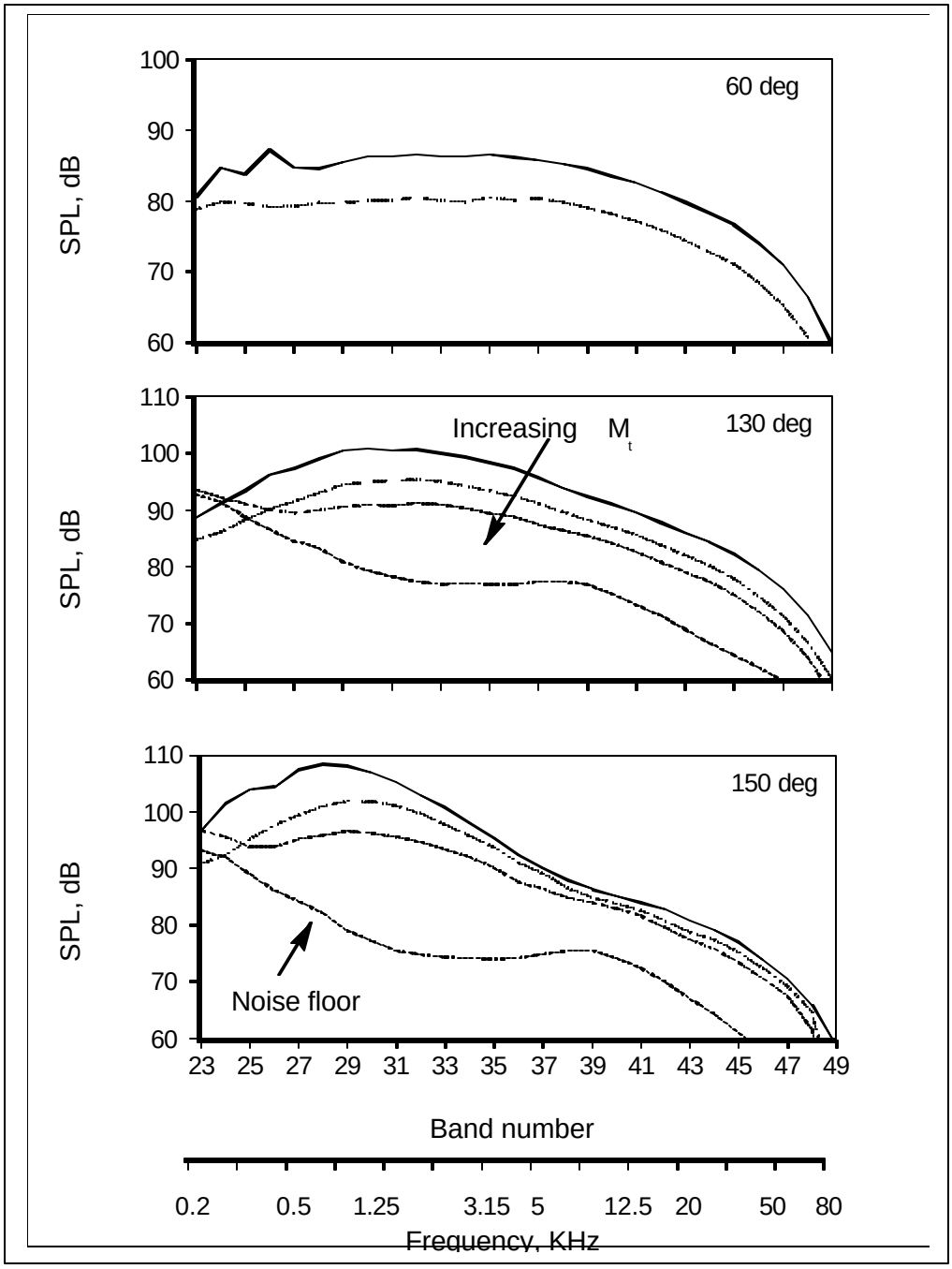

Figure A10. Effect of forward flight. NPRp=1.6, Tp/Ta=2.26, NPRs=1.8. Solid: Mt=0.0; dotted: Mt=0.2; dot-dashed: Mt=0.32; long-dashed: tunnel noise floor with Mt=0.32.

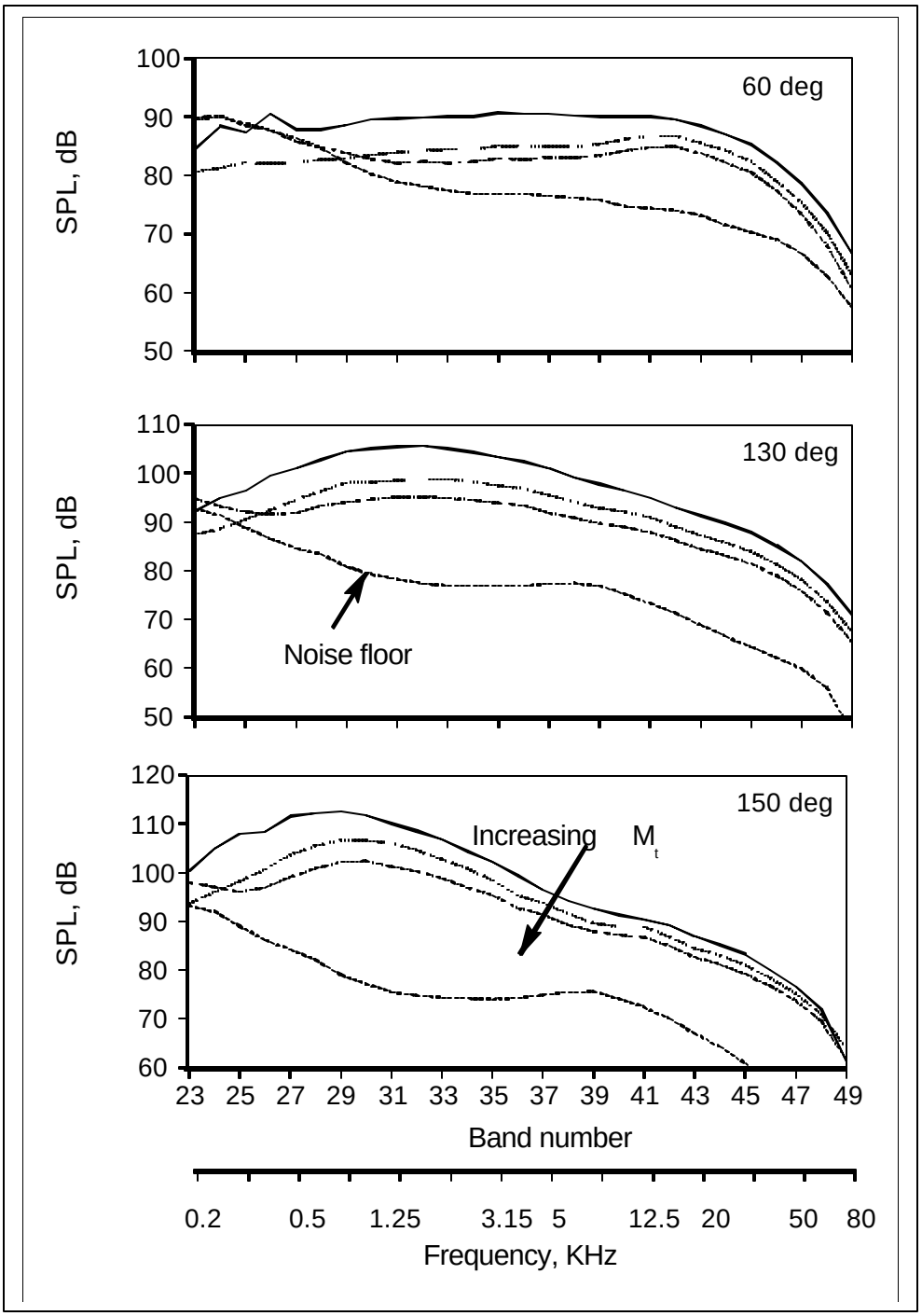

Figure A11. Effect of forward flight. NPRp=1.8, Tp/Ta=2.37, NPRs=2.1. Solid: Mt=0.0; dotted: Mt=0.2; dot-dashed: Mt=0.32; long-dashed: tunnel noise floor with Mt=0.32.